The influence of shear layer control on DDT

D.I. Baklanov,* T.A. Bormotova,† V.V. Golub,‡ A.A. Makeich,§ V.V. Volodin§

Russian Academy of Sciences, Moscow 127412, Russia

J.M. Meyers,¶ and F.K. Lu**

University of Texas at Arlington, Arlington, Texas 76019–0018

An investigation into the shear layer control of impulsive jets was carried out by comparing of different types of nozzles that were used as injectors in detonation experiments. High-speed schlieren images of the non-reactive air flow from a supersonic nozzle, a whistler nozzle and a sonic generator captured the evolution of the flow features and allowed the acoustic wave frequency to be determined. The contact surface area was calculated for the injectors. Under the same initial conditions, the contact surface areas from the different configurations are strongly different. Different injectors were mounted in turn to the injector block of a detonation tube. The flame front, shock, detonation and retonation waves were observed via pressure transducers and photodetectors. A detonation wave was observed at equivalence ratios of 0.5–2.3 for whistler and supersonic nozzles but not for sonic generators within a distance of less than 4 tube diameters.

Introduction

The quantitative prediction of the deflagration-to-detonation transition (DDT) in energetic gases is one of the major unsolved problems in combustion and detonation theory. The transition process is an extremely interesting and difficult scientific problem because of the complex nonlinear interactions among the different contributing physical processes, such as turbulence, vorticity, shock interactions and energy release.[1,2] Reduction of the DDT length is especially important in developing pulsed detonation devices that must be compact and portable.[3] The ability to mix the reactants efficiently is aggravated in pulse detonation propulsion where the mixing time is extremely limited by the high cycle rate. Thus efficient means for mixing within the detonation chamber must be developed to ensure good engine performance, such as repeatability of the detonation process.

The existence of large structures in the shear layer and their relation to flow instability make it possible to control the development of the shear layer and thus affect its mixing characteristics. The improved mixing would promote detonations and thus reduce the DDT length. Mixing enhancement techniques may be arranged in two categories depending on the way that the shear layers are manipulated, namely, passive and active.

Passive Mixing Enhancement

Gutmark et al.[4] forced a fully expanded Mach 2 circular jet using open rectangular and semicircular cavities mounted adjacent to the jet exit plane. Flow visualizations showed organized large-scale structures downstream of the cavity. The shear layer growth rate was increased by a factor of three relative to the unforced case. The observed forcing frequencies can be explained by either a convective-acoustic feedback mechanism or normal mode resonance of the cavity. The amount of increase in the shear layer growth is strongly dependent on the forcing frequency. Noncircular nozzles such as triangular or square sections have both flat sides and corners that are beneficial in combining large-scale mixing at the flat sides with small-scale mixing at the corners. Because the spreading rate at the flat sides is larger than at the corners, axis switching occurs. The small radius of curvature at the corners induces vortex deformation. The corner vortices eventually evolve into streamwise vortices. The ensuing complex vortex interaction results in improved large- and small-scale mixing.

Active Mixing Enhancement (Acoustic Driver)

The efficiency of external acoustic excitation of a high subsonic jet was demonstrated using an elliptic focusing radiator.[5] The jet nozzle was placed at a focus of an ellipsoidal enclosure, and a sound producing gas-generator was placed in the other focus. Maximum excitation of the jet was obtained for a Strouhal number between 0.25 and 0.3.

The above observations suggest that the high-speed mixing layer from a supersonic jet can be acoustically excited. The aim of this investigation is to observe the

*Leading Scientist, Institute for High Energy Densities.
†Senior Researcher, Institute for High Energy Densities.
‡Head, Physical Gasdynamics Department, Institute for High Energy Densities.
§Graduate Research Assistant, Institute for High Energy Densities.
¶Graduate Research Assistant, Mechanical and Aerospace Engineering Department. Student Member AIAA.
**Professor, Mechanical and Aerospace Engineering Department, and Director, Aerodynamics Research Center. Associate Fellow AIAA.

mixing and acoustic characteristics of impulse jets from different types of injectors. A comparison of the deflagration-to-detonation transition for these injectors was made as well.

Experiments

Injectors

The injectors were designed to produce strong acoustic disturbances. Schematics of the nozzles are shown in Fig. 1. The supersonic nozzle (Fig. 1a) produces a Mach 2 flow. The whistler nozzle (Fig. 1b) consists of a nozzle and resonator (annular cavity). The supersonic jet from the nozzle interacts with the cavity to excite instability modes in the jet. The modes depend on the jet velocity and the dimensions of the collar. The acoustic driver (Fig. 1c) consists of a sonic nozzle and resonator. The distance between the nozzle and the resonator can be adjusted by a threaded rod. The sonic generator is obtained by removing the resonator.

Flow Visualization

Experiments were carried out to visualize flow from the injectors using air as the working fluid. These experiments were simplified compared to subsequent detonation experiments in that only the flow from a single injector was visualized. The contact surface was considered to be the mixing surface between the injected and surrounding gases.

The equipment consisted of a square-section shock tube connected to a vacuum chamber that was equipped with optical windows, Fig. 2. At the end of the shock tube, different injectors were mounted in turn. The test flow was visualized by the IAB-451 schlieren system. The schlieren images show the evolution of the flow process at intervals of 5–10 μs. with an exposure of 1 μs. To obtain 72 images in one experiment, a high-speed optical-mechanical device VSK-5, with a frame size of 16×22 mm^2 was used.

The initial pressure P_0 and incident shock Mach number M_0 defined the test conditions. The mass flux through the injectors was adjusted to be equal to that calculated for the subsequent detonation experiments. Thus, the incident shock Mach number was set to obtain the same mass fluxes. Pressure ratios were 3.5 – 17.

Detonation Wave Formation

Experiments were carried out in an 83 mm diameter by 660 mm long detonation tube (6), Fig. 3. connected to a receiver (12). Injectors were mounted on an injection block (5) at the closed end of the detonation tube. Different injectors were mounted in turn on the injection block: supersonic nozzles, whistler nozzles, nozzles with radial injection and sonic generators. These injectors had the same critical area S_o = 28 mm^2.

Hydrogen and oxygen were supplied via pressure accumulators (2) at room temperature, fed from storage cylinders (1) under high pressure. The accumulators supplied calculated mass flux due to large diameters of connecting tubes under not high pressure. After the valves (4) opened, the gases completely filled the detonation chamber to 1 atm through the injectors mentioned above to obtain pre-determined equivalence ratios of ER = 0.5, 1, 2 and 2.3. The mass flux was determined to an accuracy of 15 percent. The equivalence ratio was calculated as an average value inside the tube not taking into account the ambient air mixing with the pre-combustion products during filling time. The valves remained open during and after ignition.

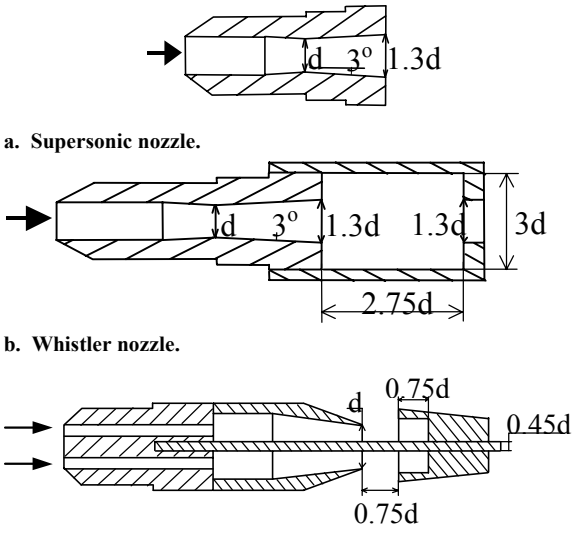

a. Supersonic nozzle.

b. Whistler nozzle.

c. Acoustic driver.

Figure 1. Schematic of injectors. All dimensions are presented in terms of the diameter of critical area.

The mixture was ignited by a power supply and ignition control system (7), Fig. 4. Electrical energy was supplied using a stabilized, high voltage source by discharge via a 4 μF capacitor. The spark plug mounted near the closed end of the tube ignited the mixture 51 ± 5 ms after the valves opened. Synchronization of the experiment was through the hydrogen valve using a specially developed delay. The entire process is triggered externally.

Compression wave and flame front parameters were measured by pressure transducers (PCB 113A34) and photodetectors (FD 256). The pressure transducers (9) and photodetectors (10) were installed at the same axial locations at 87, 174, 261 and 348 mm referenced from

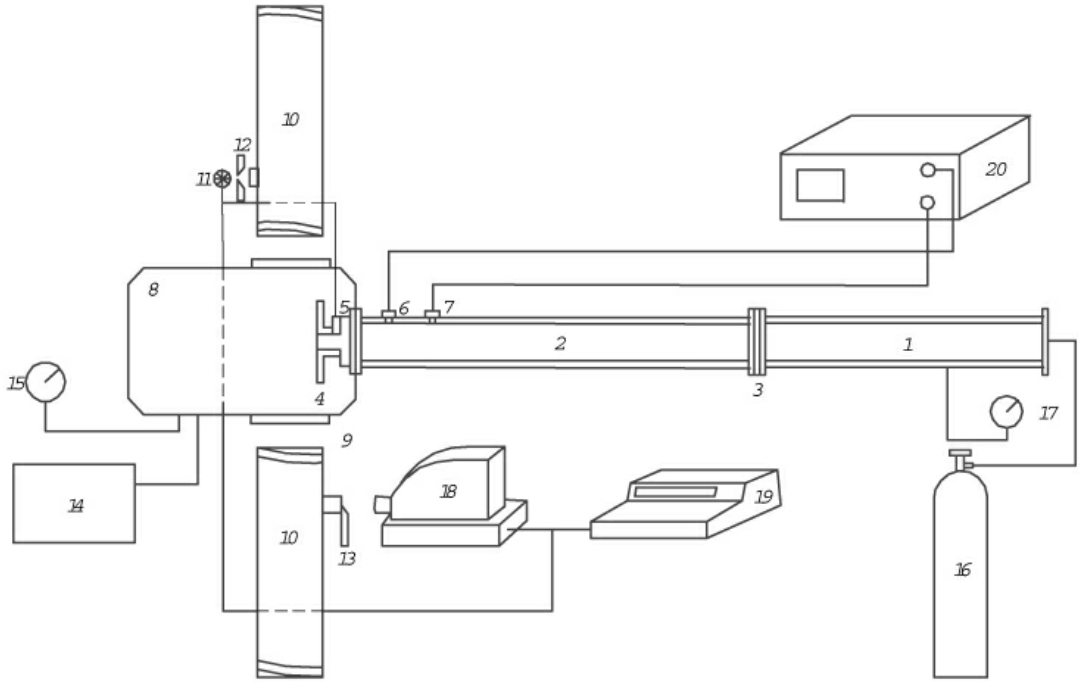

Figure 2. Flow visualization experimental setup: 1 – high pressure chamber, 2 – low pressure chamber, 3 – diaphragm block, 4 – flange with tested injector, 5, 6, 7 – piezoelectric pressure transducers, 8– vacuum chamber, 9 – optical windows, 10 – shadowgraph device IAB-451, 11 – light source, 12 – optical slit, 13 – schlieren, 14 – vacuum pump, 15 – vacuum gauge, 16 – driver gas cylinder, 17 – manometer, 18 – high speed imaging device VSK-5, 19 – VSK-5 control set, 20– oscilloscope.

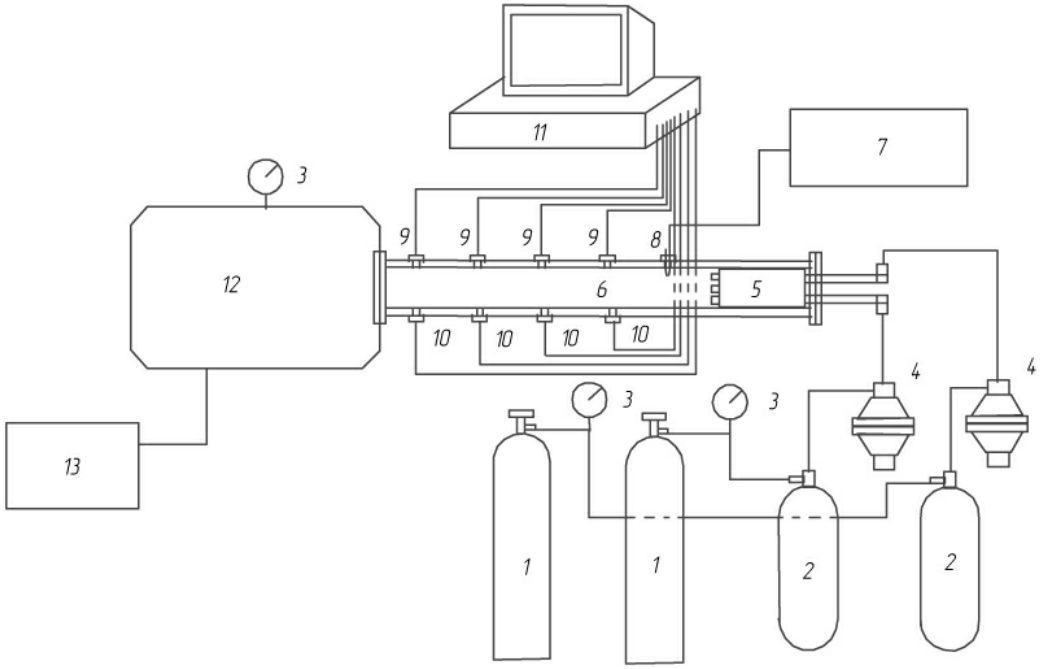

Figure 3. Experimental set-up for detonation experiments: 1 – reactant storage cylinders (hydrogen and oxygen), 2 – pressure accumulators, 3 – manometer, 4 – high mass flow valves, 5 – injection block, 6 – detonation combustion chamber, 7 – ignition power and control device, 8– spark plug, 9 – pressure transducers, 10 – photodetectors, 11 – computer equipped with oscilloscope plug-in boards, 12 – receiver, 13 – vacuum system.

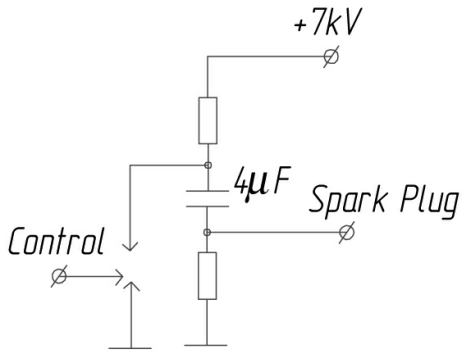

Figure 4. Schematic of ignition power and control device.

the spark plug position. Signals from pressure transducers and light gauges were recorded using a computer equipped with oscilloscope plug-in boards (11). The facility was equipped with a vacuum system (13) to remove burned gases from the detonation combustion chamber and receiver.

Results and Discussion

Flow Visualization

Whistler nozzle and sonic generator flows were visualized and evaluated. Examples of schlieren images obtained for the whistler nozzle and the sonic generator are shown in Fig. 5. The images showed that these injectors excited shear layer perturbations of the supersonic jets and produced a surrounding sound field.

Gas injection through the whistler nozzle is presented in Fig. 5a. The acoustic driver was investigated as an injector (Fig. 5b) and as an external sound field generator (Fig. 5c). The distance between the sonic generator and resonator (schematic in Fig. 1c) was chosen using schlieren images to match the acoustic frequency

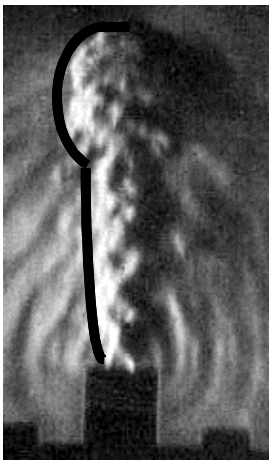

Figure 6. Whistler nozzle performance. Black line is contact surface contour that was used to calculate the symmetrical cross-sectional area of the jet plume.

closely to that of the whistler nozzle. The acoustic frequency estimated from the schlieren "movie" was 17 kHz for the sonic generator and 27 kHz for the whistler nozzle. The incident shock wave (determined from the schlieren images) increased the sound velocity due to the increase in gas temperature to about 380 K. The whistler nozzle and the external sonic generator produced an interactive sound field to excite shear layer perturbations in the supersonic jet (Fig. 5c). Figure 5c shows the breakdown of the jet from the whistler nozzle to produce a better mixing characteristic.

The contact surface marking the edge of the jet is shown by a black line in Figs. 6 and 7. The pictures were scanned into computer memory. The images were processed using Adobe Photoshop to reveal the boundaries. Since the schlieren knife-edge was installed normal to the flow direction, one side of the image appears lighter than the other. The side with the better quality

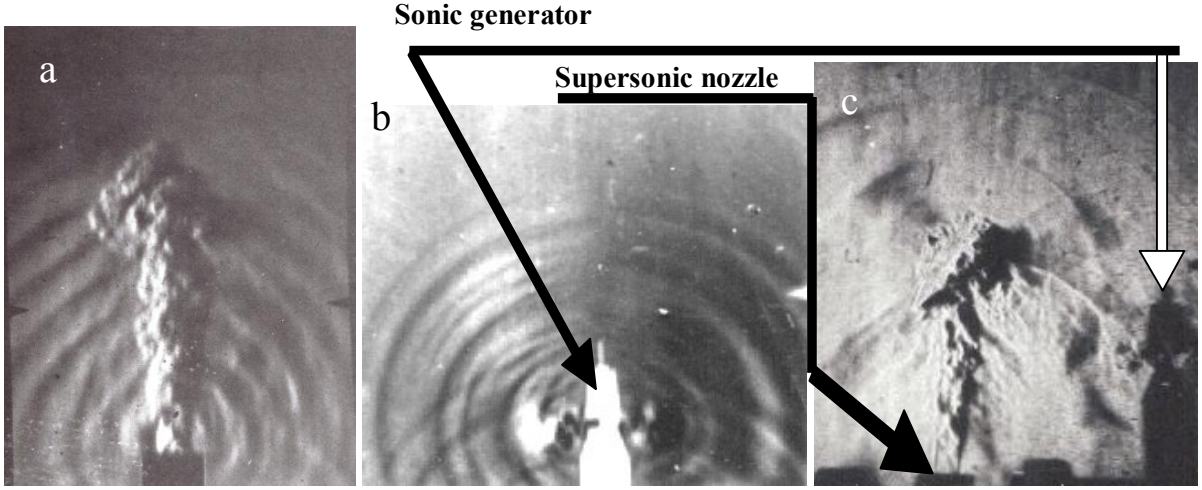

Figure 5. Schlieren images of jet flows produced by (a) whistler nozzle, (b) sonic generator, (c) whistler nozzle and sonic generator.

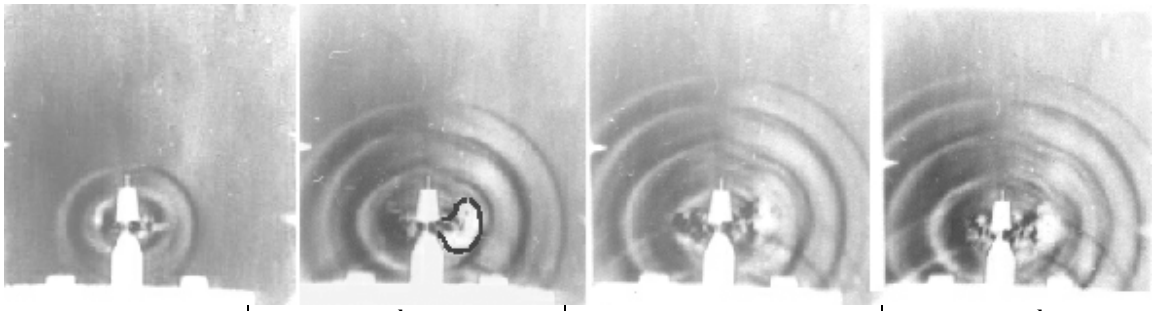

a. b. c. d.

Figure 7. Sonic generator performance. Black line is contact surface contour that was used to calculate the symmetrical cross-sectional area of the jet plume.

was chosen for defining the contact surface assuming symmetry. The boundary was then developed to obtain the surface area, using numerical integration, as a function of time.

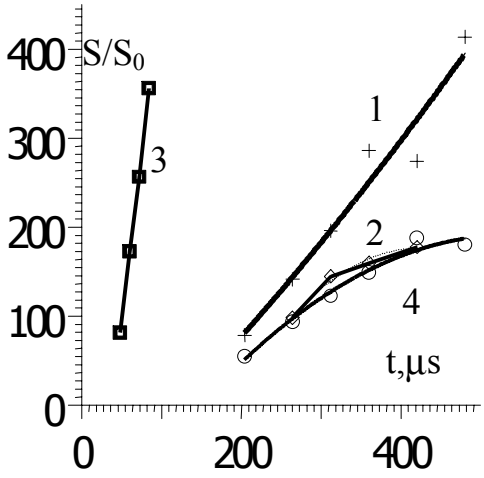

Figure 8. Dependence of the contact surface area of impulsive jets following from nozzles of the same critical area as function of time; the pressure ratio = 6.6 and mass flux of 33.1 gram/s: curve 1 – from whistler nozzle, curve 2 – from circular supersonic nozzle, curve 3 – from sonic generator, the pressure ratio = 4.05 and total mass flux = 21.1 gram/s: curve 4 – from the whistler nozzle.

The contact surface for the sonic generator became difficult to identify in later time. This is illustrated in Fig. 6, where the contact surface is clearly visible in frames *a* and *b*. Later, the contact surface became difficult to detect, see frames *c* and *d*.

The contact surface under the same initial conditions strongly differ for the whistler nozzle and nozzle without the resonator (Fig. 8, curves 1 and 2 correspondingly). This difference is increasing in time. The disturbed jet contact surface area corresponds to that of a undisturbed jet of less mass flow and pressure ratio (curve 3). The contact surface area of the sonic generator flow (curve 4) appears to exceed those of the other nozzles and conditions. The mass flows through the nozzles are included in the figures and were set equal to the calculated values in the subsequent detonation experiments.

Deflagration-to-Detonation Transition

Figure 9 shows pressure and luminosity measurements for the four locations with ER = 2.3. The figure shows the trends of the main features. The shock wave (SW) and flame front (FF) were detected in pressure and photodetector recordings correspondingly and displayed in atmospheres and volts (left and right axes in Fig. 9b respectively). The retonation wave was detected much later than the initial pressure and luminosity peaks as a following pressure peak (curve RW in Figs. 9a and b), which propagates upstream toward the closed end of the detonation tube. In section 3, the time difference between the shock wave and the flame front is 9 μs for whistler nozzles (Fig. 11b). Deflagration-to-detonation transition appears to have occurred between stations 3 and 4. Only in the fourth section was the detonation wave confirmed from luminosity and pressure measurements.

Pressure and luminosity measurements at the second section (174 mm downstream of the spark plug) for supersonic and whistler nozzles, and sonic generators are shown in Figs. 10a–c respectively for ER = 2.05. The flame front accelerations decreased for the respective injectors. The pressure peak is higher for whistler nozzle injectors than for supersonic nozzles (Fig. 10a,b) but the propagation time is less for the supersonic nozzles. The pressure peak for the sonic generators propagates much slower than for the other types of injectors (Fig. 10c).

The average velocities along the tube length were calculated for each type of injector and shown in Fig. 13 for ER = 0.5, 1.0, 2.05 and 2.3. For ER $\leq$ 1.0, the average velocities were found to exceed the calculated Chapman–Jouguet (CJ) values. However, the experimental values of peak pressures were less than calculated values. For ER > 1.0, it possible to observe pressures higher than CJ even when velocities were less than CJ. For the range of ER, the peak pressures obtained with whistler nozzles are much higher than for supersonic nozzles. For sonic generators, the velocities of the shock

wave and flame front decreased after the second section and the pressure did not reach the CJ value. These indicate that there was no transition to detonation for reactants injected by the sonic generators.

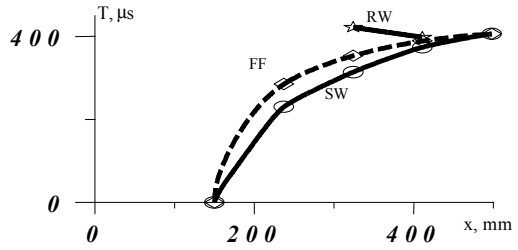

a. Wave diagram: SW = the shock wave propagation, FF = flame front propagation, RW = retonation wave propagation.

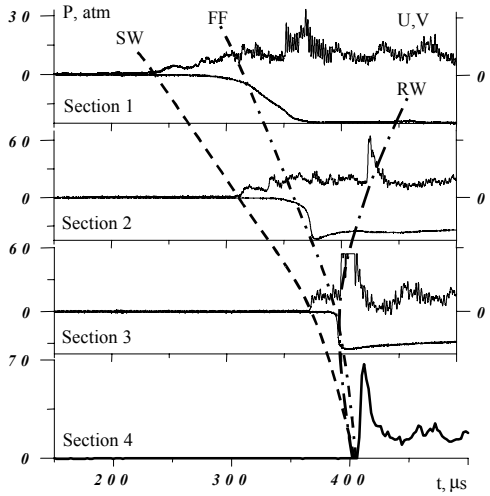

b. Pressure and luminosity data at four consecutive sections situated at 87, 174, 261 and 348 mm from the spark plug position (top to bottom).

Figure 9. Results for ER = 2.3 injected from whistler nozzles.

The two reasons can be found to extinguish DDT for sonic generators. First one is strong sound field that can quench the flame front and another one is the flow velocity in the direction of flame front and shock wave propagation. The fundamental investigations in these areas should be developed and applied for future researches.

Conclusions

The deflagration-to-detonation transition was investigated for different types of injectors. Preliminary flow visualization with air showed differences in the manner that the mixing layers developed. The jet from the supersonic nozzle in the presence of the sonic generator is highly disturbed by the acoustic field. The whistler nozzle showed superior performance in terms of rapid breakup of the gas jet.

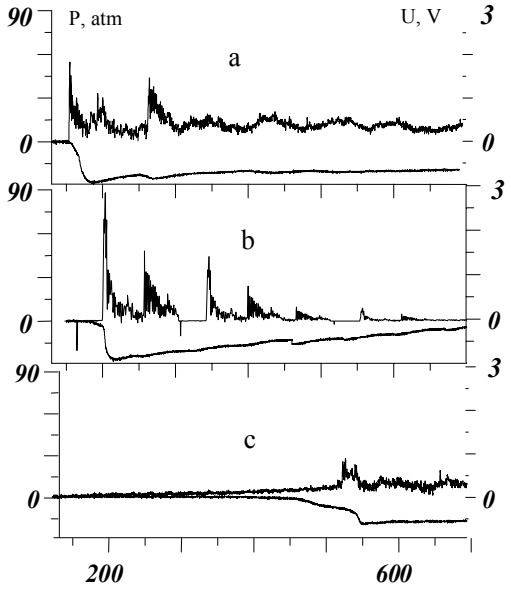

Fig.10. Pressure transducer and photodetector histories for (a) supersonic nozzle, (b) whistler nozzle and (c) conic generators respectively at section 2 for ER =2.05.

In detonation experiments with oxygen and hydrogen in a range of equivalence ratios from 0.5 – 2.3, the whistler nozzle showed the best performance, being able to achieve detonation in less than four tube diameters. The sonic generator at fuel-rich conditions did not produce flame acceleration.

Acknowledgements

This research was partly supported by U.S. Civilian Research & Development Foundation (CRDF) grant No. RE 2-22-28 and by the State of Texas Advanced Technology Program grant No. 003656-0198.

References

1. Nettleton, M.A., "Recent Work on Gaseous Detonations," *Shock Waves*, Vol. 12, No. 1, 2002, pp. 3–12.

2. Thomas, G.O. and Bambrey, R.J., "Some Observations of the Controlled Generation and Onset of Detonation," *Shock Waves*, Vol. 12, No. 1, 2002, pp. 13–21.

3. Kailasanath, K., "Applications of Detonations to Propulsion: A Review, "AIAA Paper 99–1067.

4. Gutmark, E.J., Schadow, K.C. and Yu, K.H., "Mixing Enhancement in Supersonic Free Shear Flows," *Annual Review of Fluid Mechanics*, Vol. 7, 1995, pp. 375–417.

5. Borizov, Y.Y. and Gybkina, N.M., "Acoustic Excitation of High-Velocity Jets," *Soviet Physics – Acoustics*, Vol. 21, No. 3, 1975, pp. 230–233.

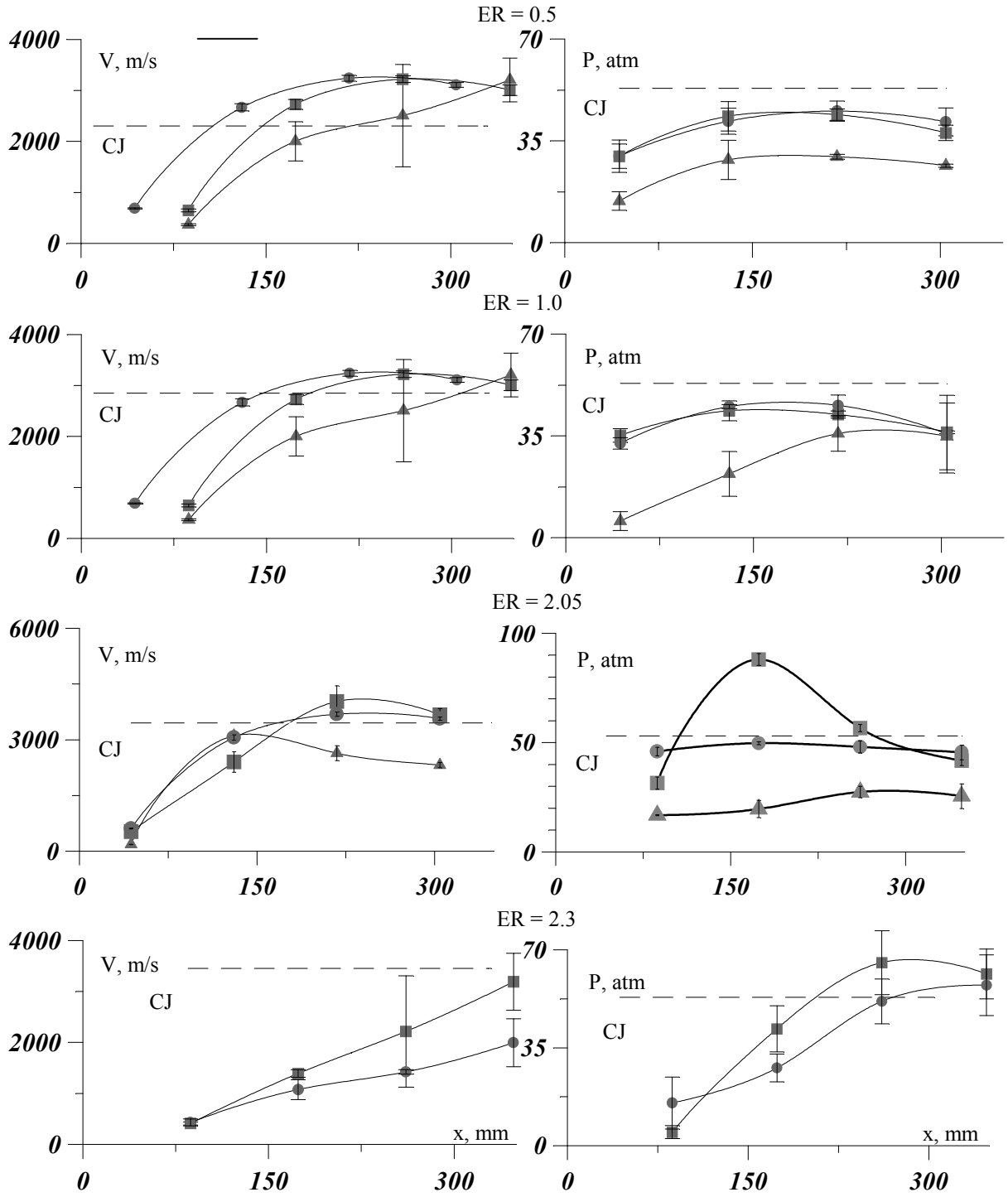

Figure 11. ER = 0.5, 1.0, 2.05 and 2.3 (from top to bottom) mixture injected from supersonic nozzles (circles), whistler nozzles (squares) and sonic generators (triangles); average velocities (left) and compression wave pressures (right).